© Universiti Tun Hussein Onn Malaysia Publisher's Office

IJIE

Journal homepage: http://penerbit.uthm.edu.my/ojs/index.php/ijie

The International Journal of Integrated Engineering

Controlling The Non-parametric Modeling of Double Link Flexible Robotic Manipulator using Hybrid PID Tuned by P-Type ILA.

Annisa J.[1,*], Mat Darus I. Z [2], M.O. Tokhi [3], A.S Z.Abidin[1],

[1]Faculty of Engineering, Universiti Malaysia Sarawak, Sarawak, Malaysia

[2]Faculty of Mechanical Engineering Universiti Teknologi Malaysia Johor, Malaysia

[3]London South Bank University, London, UK

*Corresponding Author

DOI: https://doi.org/10.30880/ijie.2018.10.07.020
Received 16 August 2018; Accepted 22 November 2018; Available online 30 November 2018

Abstract: Utilization of robotic manipulator with multi-link structure encompasses a great influence in most of the present industries. However, controlling the motion of multi-link manipulator has become a troublesome errand particularly once the flexible structure is employed. As of now, the framework utilizes the complicated arithmetic to resolve desired hub angle with the coupling result and vibration within the framework. Hence, this research aims to develop a dynamic system and controller for double-link flexible robotics manipulator (DLFRM) with the enhancement on hub angle position and vibration concealment. The research utilised neural network because the model estimation supported NARX model structure. In the controllers' development, this research focuses on self-tuning controller. P-Type iterative learning algorithm (ILA) control theme was enforced to adapt the controller parameters to fulfill the required performances once there is changes to the system. The hybrid of proportional-integral-derivate (PID) controller was developed for hub motion and end-point vibration suppression of every link respectively. The controllers were tested in MATLAB/Simulink simulation setting. The performance of the controller was compared with the fixed hybrid PID-PID controller in term of input tracking and vibration concealment. The results indicated that the proposed controller was effective to maneuver the double-link flexible robotic manipulator to the specified position with reduction of the vibration at the tip of the DLFRM structure.

Keywords: flexible robotic manipulator, Neural Network, Iterative learning algorithm, vibration suppression

1. Introduction

The wide advancement in different field of life such as domestics and industries make an incredible demand for flexible robot controller. Numerous robot controller applications are categorized as multiple-input-multiple-output (MIMO) frameworks owing to multi-link structure. The design and tuning of multi-loop controllers to meet certain conditions are regularly the pullback factors since there are interaction between the controllers. The framework must be decoupled to diminish the interaction or to form the framework diagonally dominant. Additionally, the existence of vibration on flexible structure of robot controller must be treated at the same time. The ceaseless stress delivered by the vibration can lead to structural deterioration, fatigue, instability and performance degradation. In this way, the decrease of vibration on flexible structure of robot controller is of foremost significance. In spite of the fact that numerous analysts

*Corresponding author: jannisa@unimas.my

have effectively produced the controllers for multi-link adaptable controller, the control scheme developed includes complex mathmatics to solve the coupling effect and vibration concurrently. As a result, it consumes a lot of time in numerical computation which leads to higher computational price. In this way, the disadvantage grown considerable attention in arrange to cater upcoming industries request in different applications. On-going investigation focused on improving the control strategies to satisfy all the conflicting prerequisites.

The study of adaptive controller in flexible manipulator remained until today due to its significant contribution in actual plant. Among them, a new Nonlinear Adaptive Modal Predictive Controller on two link flexible manipulator with various payload was carried out [1]. The controller could generate appropriate adaptive torque to control tip trajectory tracking and fast suppression of tip deflection. Besides, indirect control of Self-Tuning PI controller of two link flexible manipulator tune by Neural Network was proposed [2]. Simulation results showed that the tuning parameters obtain could suppress the vibration and track the desired joint angles effectively. E. Pereira et al. have investigated the use of adaptive input shaping using an algebraic identification for single-link flexible manipulators with various payloads [3]. Experiment results proved that the proposed control managed to follow tip trajectories in shorter time. Another research on adaptive controller was comprised of a fast on-line closed-loop identification method combined with an output-feedback controller for single link flexible manipulators [4]. Experimental results showed that the controller manage to follow the trajectory tracking. From the literature, it showed that there is no research using Self Tuned Controller (STC) based on ILA for double link flexible manipulator (DLFRM). This STC is very useful because it can be used effectively in handling payload variation attach in the system.

Another type of adaptive controller that is Iterative learning algorithm (ILA) has been implemented in different control scheme in the flexible manipulator system. For example, two phase ILA controllers to carry out the ideal input and output signals of iterative learning control (ILC) where the error is used to calculate the parameters of the PD controller by using standard least squares (LS) algorithm for the single link flexible manipulator (SLFM) [5]. Simulation results showed that the proposed controller is effective in tracking the desired trajectory over interval time. Zhang and Liu employed an adaptive iterative learning control scheme based on Fourier basis function for SLFM [6]. The simulation carried out portrayed that the controller successfully tracks the actual trajectory. Besides, genetic algorithm was applied to tune three combinations of controller for single link flexible manipulator in vertical plane motion that is PID, PID-PID and PID-ILC controller [7]. Simulation demonstrated that the PID-ILC parameter obtained in the optimization outperform other controllers and allow the system to perform well in reducing the vibration at the end-point of the manipulator. However, none of the research based on iterative learning algorithm (ILA) was implemented on DLFRM.

Apart from that, ILA has been utilized completely different control building issues such as robot controller for industry and healthcare, machining machine, process plant, power plant, nanotechnology region etc. Among them, Jain and Garg have proposed ILC for the nano-positioning framework to dismiss unsettling influences [8]. It has been found in simulation outcome that the controller is able to provide exceptionally disturbance rejection and the framework overshoot is decreased to worthy level. Besides, a back-stepping versatile iterative learning control joining fuzzy neural network was implemented to surmise the unidentified and robust learning term to compensate the uncertainty of robotics systems with repetitive errand [9]. Simulation outcomes appeared that the controller allow a good tracking execution for both joint position and joint acceleration. Iterative learning control (ILC) is a well-established method for control of repetitive processes. Any system offer the repetitive process opts to used ILC as a controller. The iterative learning algorithm have the same arrangement whereby it offers a simple structure with repetitive algorithm. Thus, it allows it to be easily implemented for online setting which is needed for further research in in DLFRM.

Mola et al. displayed a modern intelligent robust control strategy based on an active force control (AFC) procedure for anti-lock brake system (ABS) [10]. It is outlined and realized in a hybrid shape that's by having the iterative learning active force control (ILAFC) with a self-tuning fuzzy logic PID based (FL-PID) for successful in general execution. The significant improvement and strong performance appeared by the scheme offer the platform to persevere the research in a viable and real-time framework. Another research employed PID dynamic vibration controller utilizing ILA for marine riser whereby ILA was utilized to optimize the value of PID parameters based on the error depict within the framework [11]. Simulation comes about shown that parameters get by the ILA allow the diminishing of vibration due to vortex shedding behind the show riser pipe. A novel strategy to control mobile manipulator was developed where ILA is combined with active force control (AFC) and PID structure to compensate the dynamic effect of the unsettling influences that incorporates affect constrain and vibratory excitation connected to each wheel and joint of versatile controller [12]. Outcome exhibited that the ILC has significantly improved the general execution of the framework in decreasing the track error. The assortment of application of ILA appeared in literature review has demonstrated the competency of ILA particularly in managing with non-linear system.

In this paper, P-Type ILA in tuning the hybrid PID controller is formed. The dynamic model of the framework is created through system identification utilizing Neural Network. NARX model structure based on multi-layer perceptron is utilized to get the non-parametric modeling in comparison to Elman neural network. The control structure of PID controllers optimize by P-Type ILA is proposed for desired position and end-point vibration concealment. Performances verification of the proposed controllers are executed through simulation in MATLAB/Simulink environment.

2. Modeling and System identification

2.1 Experimental Setup and data collection

The planar DLFRM is developed and fabricated to apprehend the angular movement of manipulator as shown in Fig. 1. The schematic diagram of the framework is displayed in Fig. 2. Table I shows the physical parameters of the DLFRM system.

Table I - Parameter of DLFRM System

Parameter	Link 1	Link 2
Link Dimension (LxWxH)	0.5m×0.002m×0.041	0.5m×0.001m ×0.041
Density (ρ)	2710kg/m^3	2710kg/m^3
Modulus of elasticity (E)	7.11x1010 N/m2	7.11x 10^{10} N/m^2
Link 2nd moment of inertia	2.80 x 10^{-11} m^4	3.50 x 10^{-12} m^2
Rotor Moment of Inertia	142 gcm^2	33.5 gcm^2

Fig. 1 - Double Link Flexible Robotic Manipulator rig

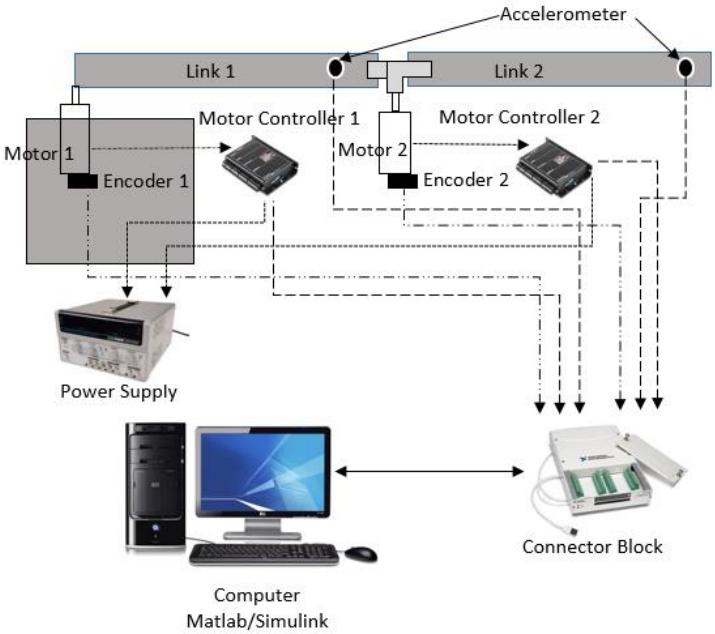

Fig. 2 - Schematic Diagram of DLFRM

The experimental study and impact test were conducted on the developed model as shown in Fig. 3 to identify the mode frequencies of the flexible links. The results of the first three modes of vibration from the experimental output and impact test of each link were compared for validation purposes. From the experiment, the frequency response for links 1 and 2 are identified. The platform to collect the data was developed via Simulink as shown in Fig. 3. Each link was knocked at 5 different points of the plain surface by a hammer or load. The tool was allowed to swing freely from a certain altitude. The dynamic responses were collected by accelerometers. The period of 9 s with sampling time of 0.01 s was set to captured and recorded the end acceleration 1 and 2. The values obtained were compared and analyzed using MATLAB software.

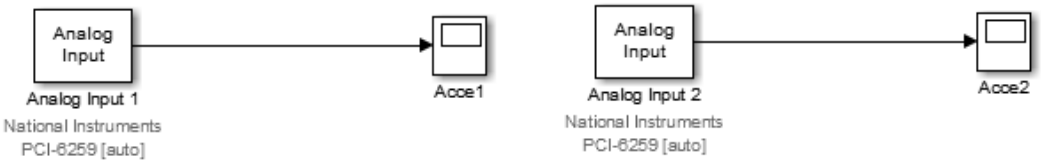

(a) Link 1 (b) Link 2

Fig. 3 - MATLAB/Simulink for data collection of links

The endpoint acceleration of flexible manipulator response of links 1 and 2 are presented in Fig. 4 and 5 respectively. The outcomes were presented in time and frequency domain. From Fig. 4, the first three resonance frequencies first link of DLFRM system were found to be at 1.516, 3.384 and 21.84 Hz. Meanwhile, 1.56, 3.229, 13.57 Hz were identified from Fig. 5 as the first three resonances of the second link of DLFRM system. It was noticed that the mode of vibration for links 1 and 2 are similar in range for the first two modes. This could be due to the presence of interaction of links 1 and 2 in the system. Though there is a connector block in between the links that segregate the first and the second link, the system could behave as a single link because the same material is used for both links. Thus, this may lead to the same characteristics and show similar behavior.

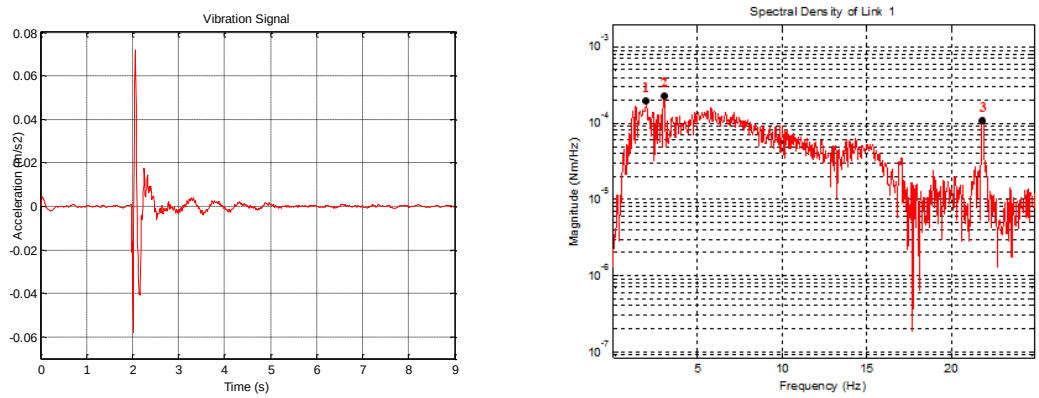

(a) Time domain (b) Frequency domain

Fig. 4 - Impact test in time and frequency domain for link 1

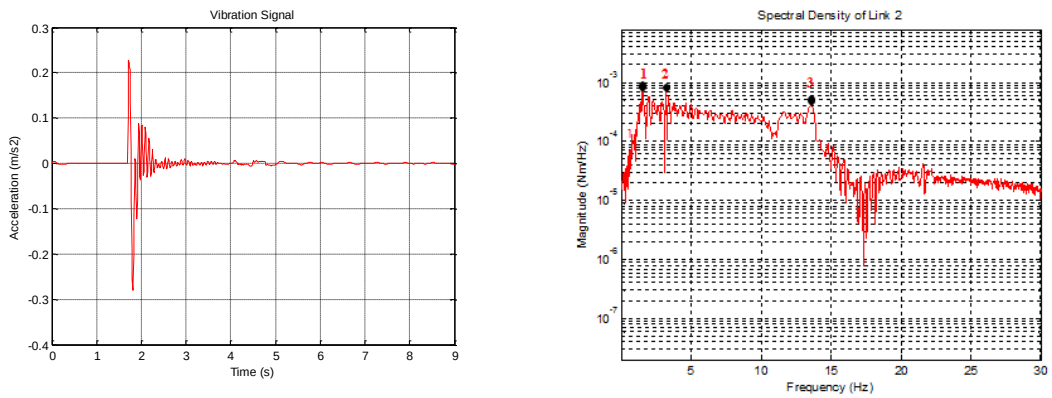

(a) Time domain (b) Frequency domain

Fig. 5 - Impact test in time and frequency domain for link 2

The data collections on the DLFRM system were carried out through the experiment. The DLFRM system was inclusive of all the sensors and actuators that were bonded at the link structure. The verification on the results obtained was conducted through the impact test. The results obtained from the impact test was then compared comprehensively with the frequency response of the system. Table II and III represent the results from the experimental test in comparison with the impact test for links 1 and 2 respectively. The impact test results are taken as a reference value. It was found that a sensible accurateness was acquired from experimental test aimed at the first three modes of vibration. The results show an acceptable percentage of error that is below 5 per cent which referred to three modes of vibration.

Table II - Summary of the calculated and experimental frequency for link 1

Resonance Mode	Impact Test (Hz)	Experiment (Hz)	Percentage of Error (%)
1	1.516	1.524	0.53
2	3.384	3.441	1.68
3	21.84	20.84	4.58

Table III - Summary of the calculated and experimental frequency for link 2

Resonance Mode	Impact Test (Hz)	Experiment (Hz)	Percentage of Error (%)
1	1.56	1.524	2.31
2	3.229	3.302	2.26
3	13.57	13.86	2.14

The comparative study concluded that the experimental work and impact test having a good agreement between them. The prominent mode in the system that is first mode shows close agreement whereby the percentage errors are 0.53% and 2.31% respectively. This imply that the experiment set up to collect the input-output data were appropriate for further analysis such as system identification and active control.

In system identification analysis, a bang-bang signal with ± 0.7 V amplitude and ± 0.5 V were utilized to supply essential torque to allow movement in the DLFRM. It is expected that two encoders and two accelerometers would capture the hub angles and end-point acceleration value for each link respectively and automatically keep in the database. The sampling time 0.01s was set for 9s length to run one complete cycle of experiment.

2.2 Modeling Estimation

The DLFRM is categorized under highly non-linear, thus non-parametric modeling is preferred to model it. Among non-parametric model, Nonlinear auto-regressive with exogenous input (NARX) have the less complicated structure. NARX model constitute a standard tool in linear black-box identification that having the nonlinear generalization of the prominent Auto-regressive with exogenous input (ARX). The neural network is employed for approximating the nonlinear part of the ARX structure. The NNARX model structure regression vector is given by Eq. (1);

$$\varphi(t)=\left[y(t-1),\ldots,y(t-n_a),u(t-k),\ldots,u(t-n_b-n_k+1)\right]^T \quad (1)$$

where $\varphi(t)$ is a vector containing the regressors, where $y(t-1)$ is delayed versions of the outputs and u is delayed inputs to the system and n_a, n_b, n_k are system order and delay. The regression vector is molded of pass values of the input and output of the system. In validating the structure, one step ahead (OSA) prediction of the Neural network nonlinear Auto Regressive exogenous (NNARX) model is utilized and it is given by Eq. (2);

$$\hat{y}(t/\theta)=y(t/t-1,\theta)=g(\varphi(t),\theta) \quad (2)$$

where $\hat{y}(t/\theta)$ is the predictions output, $y(t)$ is the true outputs and g is the function formed by the neural network scheme. The back propagation for multi-layer perceptron (MLP) neural network and Elman neural networks (ENN) were applied in the research. All the four model of the DLFRM system which constitute of four Single Input Single output (SISO) were undergone both estimation process using MLP and ENN.

The developed model undergoes the verification process to optimize the model obtain. Apart from Mean Squared Error (MSE), the following Correlation Test is utilized;

$$\begin{aligned}
&\varphi_{\varepsilon\varepsilon}(\tau) = E\left[\varepsilon(t-\tau)\varepsilon(t)\right] = \delta(\tau) \\
&\varphi_{u\varepsilon}(\tau) = E\left[u(t-\tau)\varepsilon(t)\right] = 0, \forall\,\tau \\
&\varphi_{\varepsilon^2\varepsilon}(\tau) = E\left[u^2(t-\tau) - \bar{u}^2(t)\varepsilon(t)\right] =, \forall\,\tau 0 \\
&\varphi_{\varepsilon^2\varepsilon^2}(\tau) = E\left[u^2(t-\tau) - \bar{u}^2(t)\varepsilon^2(t)\right] = 0, \forall\,\tau \\
&\varphi_{\varepsilon(\varepsilon u)}(\tau) = E\left[\varepsilon(t)\varepsilon(t-1-\tau)u(t-1-\tau)\right] = 0, \tau \geq 0
\end{aligned} \tag{3}$$

where $u(t)$ and $\varepsilon(t)$ are input and residual respectively, $\varphi_{\varepsilon\varepsilon}(\tau)$ is auto-correlation of residuals, $\varphi_{u\varepsilon}(\tau)$ cross-correlation of input and residuals, $\varphi_{\varepsilon^2\varepsilon}(\tau)$ is cross-correlation of input square and residuals, $\varphi_{\varepsilon^2\varepsilon^2}(\tau)$ is cross correlation of input square and residuals square, $\varphi_{\varepsilon(\varepsilon u)}(\tau)$ is cross correlation of residuals and (input*residuals) and $\delta(\tau)$ is an impulse function. The model is developed using nonlinear structure that is NARX. Hence, it is compulsory to fulfill all the five conditions. The details of the modeling is elaborated in previous study [13].

3. Control Scheme

Fig.6 and 7 shows the separate control scheme for DLFRM. The PID_{i1} controller is developed for hub angle motion while PID_{i2} controller is applied for flexible body motion. The complete PID controllers are tuned by P-Type ILA. Each link constitutes of two loops (*i=1,2*) which both are incorporated to grant control inputs for double link flexible robotic manipulator framework.

3.1 Controller Design

In this research , the intelligent PID controllers are employed to guarantee the hub tracks the reference trajectory and the vibration of the system is eradicated simultaneously through end-point acceleration feedback.

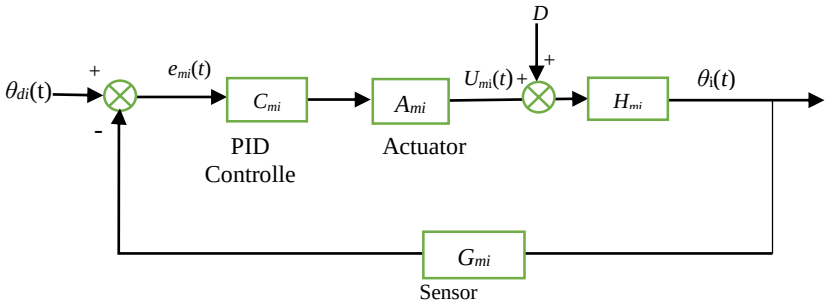

Fig. 6 - Block diagram of control rigid body motion

For the hub angle motion, θ_{di} , and $\theta_i(t)$ represents reference hub angle and actual hub angle of the system respectively. By referring to the block diagram in Fig. 6, the close loop signal of U_{mi} can be written as;

$$U_{mi}(t) = A_{mi}\left[\left(C_{mi}(t)e_{mi}(t)\right)\right] \qquad i = 1,2 \tag{4}$$

where U_{mi} is PID control input, A_{mi} is motor gain and C_{mi} is PID controller. The controller gains are K_{Pi}, K_{Ii} *and* K_{Di}. And;

$$\theta_i(t) = H_{mi} \tag{5}$$

$$H_{mi} = U_{mi}(t) + D \tag{6}$$

The error function of the system is defined as in Eq. (7);

$$e_{mi}(t) = [\theta_{di}(t) - G_{mi}\theta_i(t)] \qquad i = 1,2 \tag{7}$$

Therefore, the closed loop transfer function obtained as in Eq. (8);

$$\frac{\theta_i}{\theta_{di}} = \frac{[C_{mi}]A_{mi}H_{mi}}{1 + [C_{mi}]A_{mi}G_{mi}H_{mi}} \tag{8}$$

For the flexible motion as illustrated in Fig. 7, the control input is given by;

$$U_{pi}(t) = A_{pi}[C_{pi}(t)e_{pi}(t)] \qquad i = 1,2 \tag{9}$$

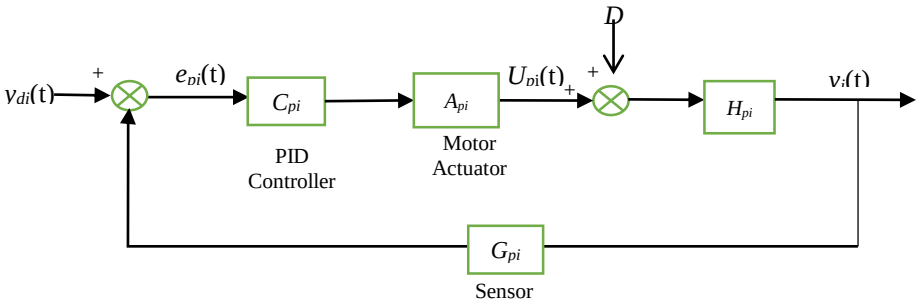

Fig. 7- Block diagram of control flexible body motion

where U_{pi} is PID control input, A_{pi}, are piezoelectric gain, C_{pi} is PID controller as derived in Eq. 9. The controller gains are K_{Pi}, K_{Ii} *and* K_{Di}. The deflection output represents by y_i and the desired deflection y_{di} is set to zero. And;

$$y_i(t) = U_{pi} \tag{10}$$

$$H_{pi} = U_{pi}(t) + D \tag{11}$$

Thus, the error e_{pi} is defined as;

$$e_{pi}(t) = [0 - G_{pi}y_i(t)] \qquad i = 1,2 \tag{12}$$

Therefore, the closed loop transfer function obtained as;

$$\frac{y_i}{y_{di}} = \frac{[C_{pi}]A_{pi}H_{pi}}{1 + [C_{pi}]A_{pi}G_{pi}H_{pi}} \tag{13}$$

The acceptable performance of DLFRM rely on U_{mi} and U_{pi} in which extremely depended on the tuned parameters, K_{Pi}, K_{Ii} and K_{Di} that being fed to the system. The performance of the PID controller of hub angle was determined by transient performance such as hub angle settling time, overshoot, rise time and steady state error. Meanwhile, the performance of the PID controller of vibration suppression was determined by means of the MSE value. The lower value of those parameters indicates the good control outcome.

3.2 P-type ILA

Iterative learning algorithm is a scheme that employ data in past repetitions to improve the control signal which eventually empowering an appropriate control action. ILA gives prevalent performances without intemperate on control-loop feedback. The research focuses on utilizing the ILA to improve the performance of PID control structure. Hence, ILA act like an intelligent mechanism in which the response of a dynamic system improves as time increases based on

some error criterion. This is categorized under adaptive controller which solves the problem of fixed controller. Fig. 8 shows the details of schematic diagram of the ILA tuned by PID controller.

The scheme put forward the concept of self-tuning of the PID controller parameters by ILA to lessen the whole error in the system to facilitate the performance. The equation employed is presented in the following [14]:

$$\begin{aligned} K_P(k+1) &= K_P(k) + \varphi_1 \times e(k) \\ K_I(k+1) &= K_I(k) + \varphi_2 \times e(k) \\ K_D(k+1) &= K_D(k) + \varphi_3 \times e(k) \end{aligned} \tag{14}$$

where $K(k)$ is the stored value from the previous iteration (from memory), $K(k+1)$ is the updated value (to memory), Φ_1 is the proportional learning parameter, Φ_2 is the integral learning parameter, Φ_3 is the derivative learning parameter and $e(k)$ is the system error. ILA act to compute the parameters' approximation such that the system output approaches a suitable value as the time escalate. However, the over learning might happen amid the learning forms as the time expanded ceaselessly. This condition might lead to framework precariousness when it enters a perilous zone [14]. Thus, a stopping criterion is actualized into the ILA to overcome this shortcoming.

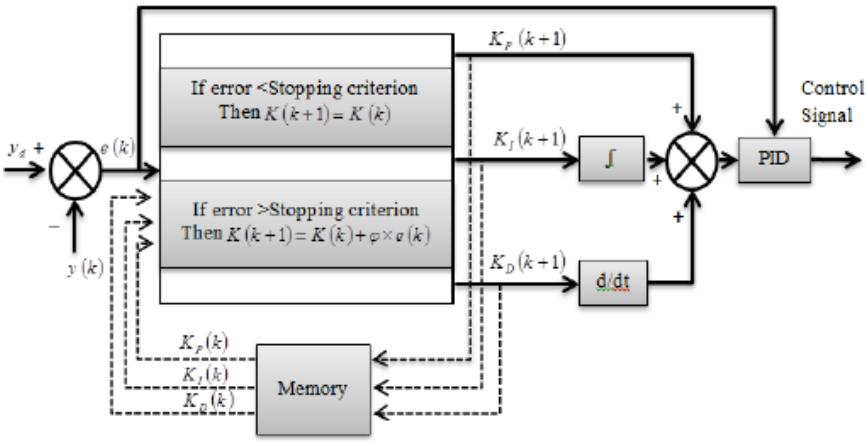

Fig. 8 - P-type ILA with PID controller

By that, the learning process will halt promptly when the stopping criterion is met. Subsequently, within the proposed controller, the PID controller parameters are upgraded at each trial concurring to the stopping criterion error. This stopping criterion is based minimum value of error function. In this study, there are two errors are considered that is to minimize the error from the hub angles and error from the end-point acceleration. The stopping criterion error for hub is set at 0.02 rad. And for end point acceleration, the stopping criterion error is set to 0.0015 m/s^2. For hub angle, the smaller value indicates precision in positioning the link to desire position. In the interim, the smaller value of end-point acceleration infers that the vibration within the framework is exceptionally much decreased. The error can be calculated by using Eq. (15)

$$e(k) = y_d(k) - y(k) \tag{15}$$

where $e(k)$, $y_d(k)$ and $y(k)$ is the system error, desired input and actual output respectively.

New signals $K_P(k+1)$, $K_I(k+1)$ and $K_D(k+1)$ are calculated based on the stopping criterion error. The new stored signals were employed in the next iteration. The new signals $K_P(k+1)$, $K_I(k+1)$ and $K_D(k+1)$ are calculated based on Eq. (11) if the error is exceeding the set stopping criterion error. However, in the event that the error is lesser than the stopping criterion error, then the new signals $K_P(k+1)$, $K_I(k+1)$ and $K_D(k+1)$ are calculated utilizing the following equations:

$$\begin{aligned} K_P(k+1) &= K_P(k) \\ K_I(k+1) &= K_I(k) \\ K_D(k+1) &= K_D(k) \end{aligned} \tag{16}$$

At this point, the iteration would halt to dodge over learning. Those values are considered the best parameters numeral for PID controller.

4. Results and discussion

4.1 NNARX Modeling

Table IV summarizes the best model and overall comparative performance for the hub angle and end-point acceleration. The result of modeling for hub angle 1 and hub angle 2 using MLP and ENN prediction structure are compared. It is observed that MLP is competent to follow the actual data closely. The error between actual and predicted MLP output almost negligible or close to zero. Meanwhile, the ENN prediction of hub angle 1 and 2 for the same data show that ENN is able to trace the actual data. However, there is critical disparity between the actual data and prediction data. The deviation is indeed more discernible on the validated data section. The error is significant and cannot be neglect. The models obtained via MLP undergo correlation test fall within 95% confidence for both links.

Table IV- Summary of the best performance achieved in modeling

	Model	Spec.	T (s)	MSE	Corr. test
MLP	**Hub1**	MS: [2 2 1], Ite: 150	3	0.0000685	unbiased
	Hub2	MS: [2 2 1], Ite: 150	3	0.000752	unbiased
	End-point Acceleration 1	MS: [2 2 1], Ite: 150	3	0.0025	unbiased
	End-point Acceleration 2	MS: [2 2 1], Ite: 150	3	0.0049	unbiased
ENN	**Hub1**	MS: [8 8 1], Ite: 150	2	0.0047	biased
	Hub2	MS: [8 8 1], Ite: 150	2	0.0023	biased
	End-point Acceleration 1	MS: [8 8 1], Ite: 150	3	0.018	biased
	End-point Acceleration 2	MS: [8 8 1], Ite: 150	3	0.015	biased

Conversely, the models obtained via ENN undergo the correlation test are clearly drop far-off 95% confidence level for both links. The same outcomes of correlation test were found in modeling of end-point acceleration for both link 1 and link 2 using MLP and ENN respectively. This appear that MLP is predominant in predicting the model as compared to ENN. The error between actual and predicted MLP output is negligible. The correlation test for end-point acceleration of both link 1 and link 2 also shows that the results of MLP model fall within 95% confidence level. Meanwhile, the correlations of the error for both models using ENN are clearly drop far-off 95% confidence level. Hence, it can conclude that both models predicted by ENN are biased.

The details of correlations test with the graph can be obtained from previous research [13]. The DLFRM model attained by means of MLP will be exploited in developing of control for hub-angle and end-point acceleration of the DLFRM.

4.2 Control Results

Simulation was carried out in order to study the effectiveness of the PID-ILA controller in trajectory tracking and vibration concealment control of DLFRM with no payloads. The simulation was realized and confirmed within MATLAB/Simulink environment. The Simulink models were constructed on block diagram shown in Fig. 9 and 10. Step signals were supplied as input reference with maximum magnitude of ± 2.1 rad and ± 1.1 rad for links 1 and 2 respectively. The learning parameters were tuned through trial and error technique. The simulations were run employing the sampling rate of 0.01 s within 9 s. The controller keeps the value of parameter gains throughout the simulation process. These values are utilized as references within the next parameter gains' computation which is recognized by error discrepancy.

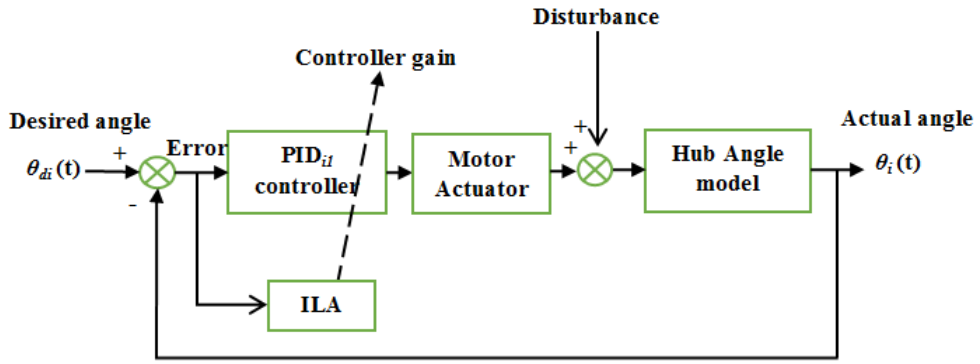

Fig. 9 - Block diagram of self-tuning control scheme based on ILA for hub angles 1 and 2

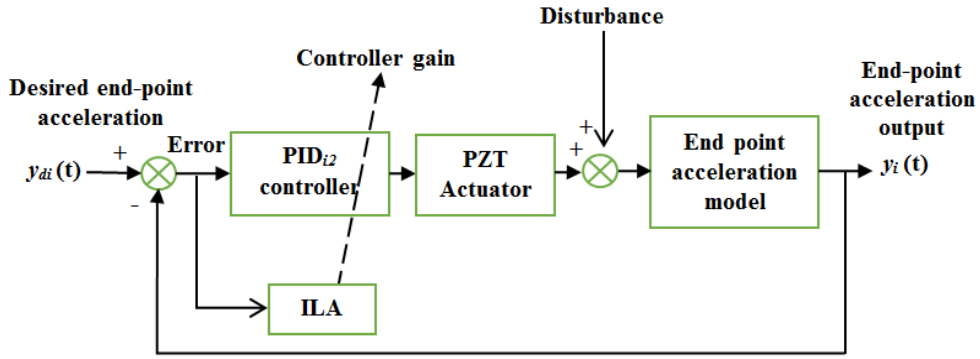

Fig. 10 - Block diagram of self-tuning control scheme based on ILA for end-point accelerations 1 and 2

4.2.1 Hub angle Motion

Amid the simulation, the learning process was executed to discover a new controller parameter based on the learning parameters. The learning parameters exhibited in Eq. (14) were tuned through trial and error method. The learning parameters were set to $\Phi 1$ = 3, $\Phi 2$ = 1 and $\Phi 3$ = 10. The controller keeps the value of parameter gains and utilizes these values as references for the next cycle. The next parameter gains are identified by error discrepancy. The control parameters of K_P, K_I, and K_D converge when it obtained the constant values as appeared in Fig. 11.

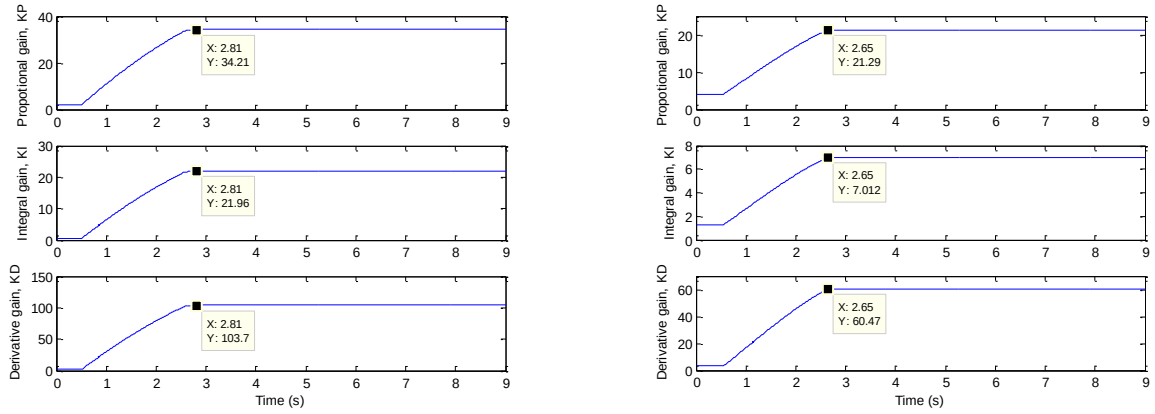

Fig. 11- (a) Parameters convergence of hub angle 1 using PID-ILA controller; (b) Parameters convergence of hub angle 2 using PID-ILA controller

At this point the minimum output error is reached. The parameters K_P, K_I, and K_D of both links become settle at about 2.81 s and 2.65 s respectively.

The intelligent PID-ILA controller was compared with the fixed controller, PID-PSO. PID-ZN worked as the control benchmark. The simulation step response for closed-loop hub angle 1 and 2 of PID-ILA controller at stopping criterion error of 0.02 rad are shown in Fig. 12 and 13 with initial values of K_p =2.083, K_I = 0.539 and K_D= 2.010 and K_p =4.148, K_I = 1.296 and K_D= 3.318 for links 1 and 2 respectively. These values were found through Ziegler-Nichols method

conducted in previous research [15]. The stopping criterion value was attained through trial method. The parameter will converge exceptionally quick up to the extent that the link yet to reach desired angle. In any case, in the event that the esteem is too small the parameter will never converge. The impact of integrating the iterative learning to the framework can be examined as the error between the actual and desired angle converges to a minimum value as time rises. The iterative term within the controller will iterate until it reaches the least output error. In case the least yield error is reached, the parameter gains for the controller will become steady over time. The performance of self-tuning PID-ILA control structure is observed in terms of rise time, t_r (s), settling time, t_s (s), maximum overshoot, M_p (%) and steady state error, E_{ss} (rad).

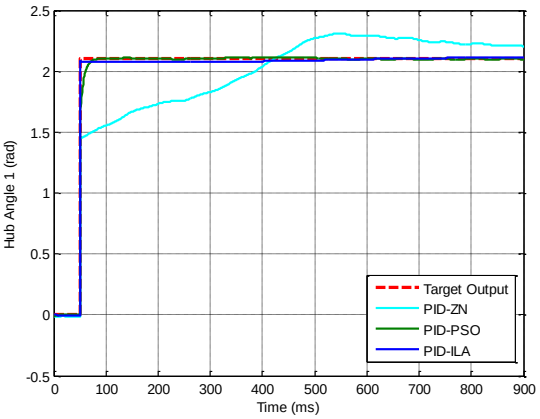

Fig. 12 - Comparison between PID-ZN, PID-PSO and PID-ILA of hub angle 1

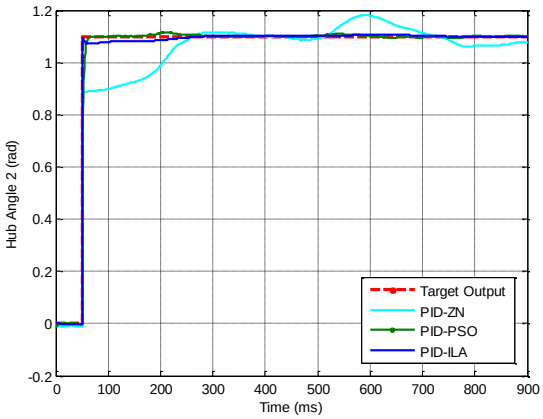

Fig. 13 - Comparison between PID-ZN, PID-PSO and PID-ILA of hub angle 2

The numerical results are tabulated in Table V. It can be observed from the outcomes that PID-ILA control structure improves the t_r, t_s and M_p compared to fixed PID control structure. Also, the results exhibited that PID-ILA control structure for link 1 and 2 were able to follow the specified hub-angle of DLFRM. There is noteworthy enhancement detected on PID-ILA. PID-ZN simply provides the starting point for further tuning. Hence, the result may not accomplish the ideal behavior. The rate of enchantment attained by PID-ILA controller compared with PID-PSO controller for t_r, t_s and M_p are 86.2 %, 44.94 % and 86.21% for link 1 and 80.95 %, 16.95 % and 17.91 % for link 2.

Table V - Performance of controllers for hub angle

Controller	Parameters of controllers						Rise Time (s), t_r	Settling Time (s), t_s	Over shoot (%), M_p	SSE, E_{ss}
	Φ_1	Φ_2	Φ_3	K_P	K_I	K_D				
HUB 1										
P-Type ILA	3	1	10	13.8	8.30	40.9	0.008	0.49	0.16	0
PID-PSO	-	-	-	3.7	57.8	3.4	0.058	0.89	1.16	0.003
PID-ZN	-	-	-	2.1	0.54	2.0	2.965	7.147	4.69	0.68
HUB 2										
P-Type ILA	3	1	10	21.3	7.01	60.5	0.008	0.49	1.10	0
PID-PSO	-	-	-	2.19	88.2	0.79	0.042	0.59	1.34	0.002
PID-ZN	-	-	-	4.15	1.29	3.32	1.460	5.45	5.45	0.21

4.2.2 Flexible Motion

The same simulation process applied to the end-point acceleration control. The learning parameters were attained by means of trial method that is Φ_1=3, Φ_2=1 and Φ_3=5 for both links. The learning process to discover the new controller parameters is executed based on the learning parameters. Fig. 14 displays the convergence value of the control parameters of K_P, K_I, and K_D when it come to the steady values. The initial value of K_p =7.2, K_I = 21.176 and K_D= 1.812 and K_p= 4.16, K_I = 55.082 and K_D= 3.052 for links 1 and 2 respectively. These values were obtained from Ziegler-Nichols strategy [15]. The value ended up consistent once the least yield error come to the set stopping criterion error that is 0.0015 m/s^2. This value also attained via trial method. In case the value is too high, the parameter will merge exceptionally quick to the degree that the vibration concealment exceptionally insignificant. However, if the value too small the parameter will

never converge. The estimated time for the controller parameters K_P, K_I, and K_D of both links to settle at those constant values are about 7.34 s and 8.27 s respectively.

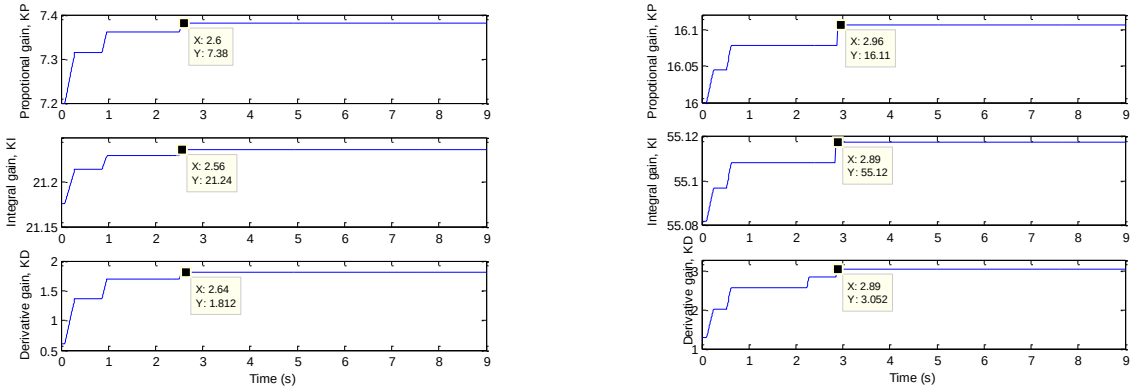

Fig. 14 - (a) Parameters convergence of end-point acceleration 1 using PID-ILA controller; (b) Parameters convergence of end-point acceleration 2 using PID-ILA controller.

The fixed controller, PID-PSO was used as the standard of assessment for the intelligent PID-ILA controller. The outcome appears to be that PID tuning through ILA managed to improve the performance of vibration suppression than those obtained by the PSO strategy. Fig. 15 and 16 show the results for both links respectively.

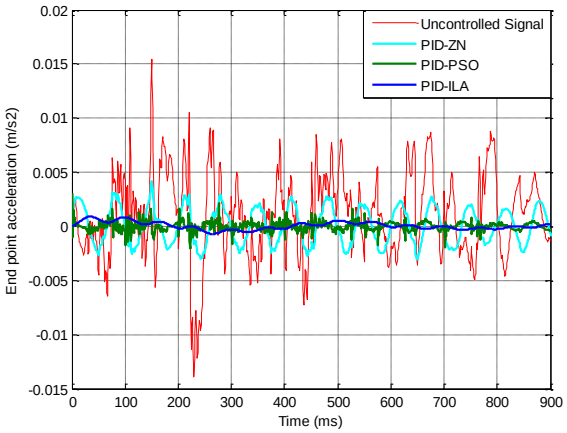

Fig.15 - Comparison between controllers for end-point acceleration 1

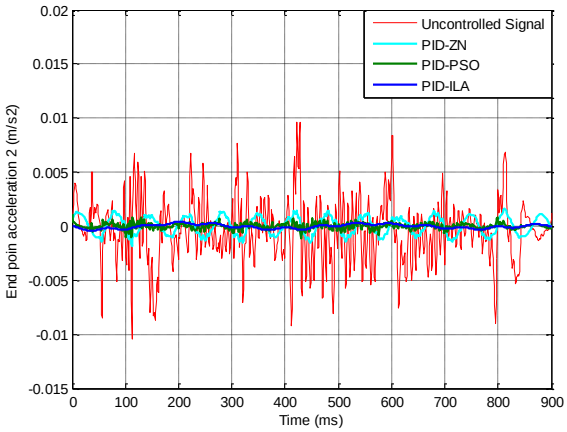

Fig. 16 - Comparison between controllers for end-point acceleration 2

Numerical results tabulated in Table VI displays that the MSE value of the PID-ILA control are recorded t the most reduce value in comparison to other controllers. The rate of improvement accomplished by PID-ILA controller compared to PID-PSO controller for MSE is 54.15 % and 6.05 % for link 1 and 2 respectively.

Table VI - Performance of controllers for end-point acceleration

Controller	Parameters of controllers						MSE	Parameters of controllers						MSE
	Φ_1	Φ_2	Φ_3	K_P	K_I	K_D		Φ_1	Φ_2	Φ_3	K_P	K_I	K_D	
	Link 1							Link 2						
PID-ILA	3	1	5	7.38	21.24	1.812	1.810×10^{-8}	3	1	5	16.11	55.12	3.052	4.054×10^{-8}
PID-PSO	-	-	-	2.07	498.1	2.33	3.948×10^{-8}	-	-	-	8.06	817.9	1.033	4.315×10^{-8}
PID-ZN	-	-	-	7.2	21.18	0.612	2.822×10^{-6}	-	-	-	16	55.08	1.281	7.564×10^{-7}

This could be further examined from frequency domain result as appeared in Fig.17 (a) and (b). The employment of PID-ILA control brings to higher attenuation value for link 1 that is 56.8 dB as compared to PID-PSO that is 44.3 dB. The attenuation value of PID-ILA for link 2 shows the same pattern is that is 38.1 dB as compared to PID-PSO that is 35.8 dB. The comparison focused on mode 1 since the first mode is mode is prevailing and contributes considerable impact to the framework.

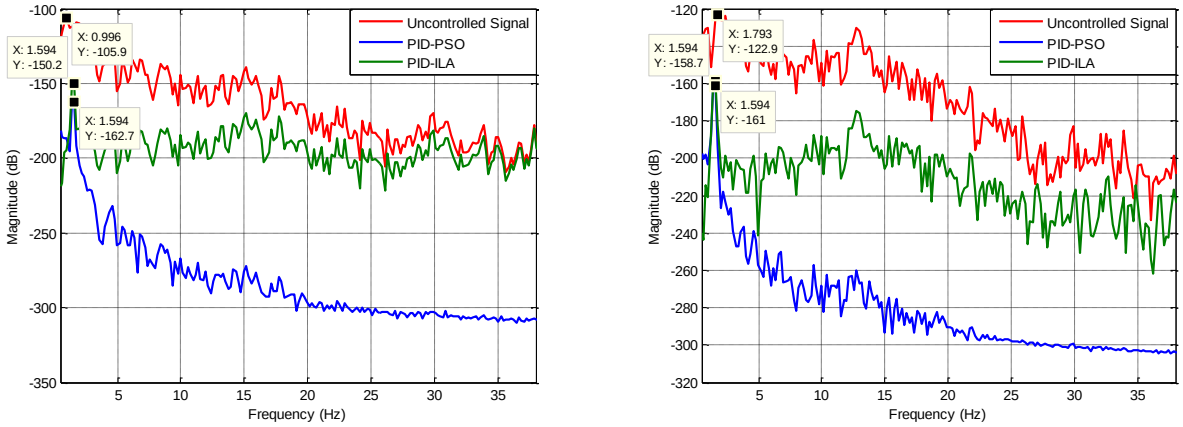

(a) Link 1 (b) Link 2

Fig. 17- Spectral density of the system output not label axes with a ratio of quantities and units.

5. Conclusions

In this work, the self-tuned control strategy was proposed for DLFRM based on the estimated dynamic model. The proposed P-Type ILA to tune the PID controller in tracking the desired hub-angle and suppress the vibration of DLFRM was investigated and compared with corresponding fixed control structure that is conventional PID and PID-PSO. The research shows that the the model structure, NARX utilizing MLP as estimator is able to supply great and solid system identification of DLFRM system. The claimed is proven through the lower MSE results and unbiased correlation test. It is noted that PID-ILA control structure performed well as compared to those fixed PID control structure specifically PID-PSO manages to give a good response. For the hub angle, the percentage of improvement achieve by P-Type ILA controller compared with PID-PSO controller for t_r, t_s and M_p are 86.2 %, 44.94 % and 86.21% for link 1 and 80.95 %, 16.95 % and 17.91 % for link 2. Meanwhile, the percentage of improvement for flexible body control achieve by PID-ILA controller compared to PID-PSO controller in term of MSE are 54.15 % and 6.05 % for link 1 and 2 respectively. It can be concluded from this observation that the performance of the proposed adaptive PID-ILA control scheme is better than the fixed PID controller.

Acknowledgement

The authors would like to express their gratitude to Minister of Education Malaysia (MOE), Universiti Teknologi Malaysia (UTM) and Universiti Malaysia Sarawak (UNIMAS) for funding and providing facilities to conduct this research

References

[1] Pradhan, S. K., and Subudhi, B., "Nonlinear Adaptive Model Predictive Controller for a Flexible Manipulator: An Experimental Study," IEEE Transaction on Control System Technology, 22(5), pp,1754–1768, 2014.

[2] Sasaki, M., Asai, A., Shimizu, T., and Ito, S., "Self-Tuning Control of a Two-Link Flexible Manipulator using Neural Networks," In ICROS-SICE International Joint Conference, pp.2468–2473, 2009.

[3] Pereira, E., Trapero, J. R., Díaz, I. M. and Feliu, V., "Adaptive input shaping for manoeuvring flexible structures using an algebraic identification technique," Control Engineering Practice, 20, pp.138–147. 2009.

[4] Becedas, J., Trapero, J. R., Feliu, V., and Sira-Ramirez, H., "Adaptive controller for single-link flexible manipulators based on algebraic identification and generalized proportional integral control," IEEE Transactions on Systems, Man, and Cybernetics Society, 39(3), pp.735–51, 2009.

[5] Mute, D., Ghosh, S., and Subudhi, B., "Iterative Learning Control of a SingleLink Flexible Manipulator Based on an Identified Adaptive NARX Model," InAnnual IEEE Indian Conference, 2013.

[6] Zain, B.A., Tokhi, M.O. and Toha, S.F., "PID-based control of a single-link flexible manipulator in vertical motion with genetic optimisation," In 2009 3rd European Symposium on Computer Modelling and Simulation, pp.355–360, 2009.

[7] Zhang, L., and Liu, S., "Basis Function Based Adaptive Iterative Learning Control for Non-Minimum Phase Systems," In World Congress on Intelligent Control and Automation, pp.828–833, 2014.

[8] Jain, S., and Garg, M., "Identification and Iterative Learning Control of Piezoelectric Actuator Based Nano-positioning System," International Journal of Advance in Engineering Sciences, 3(3), pp.88–93, 2013.

[9] Wang, Y., Chien, C., and Chuang, C., "Adaptive iterative learning control of robotic systems using back-stepping design," Transaction of Canadian Society for Mechanical Engineering, 37(3), pp.591–601, 2012.

[10] Al-Mola, M., Mailah, M., Muhaimin, A. H., Abdullah, M. Y. and Samin, P. M., "Fuzzy-based PID with iterative learning active force controller for an anti-lock brake system," International Journal of Simulation: Systems, Science and Technology, 13(3 A), pp. 35–41, 2012.

[11] Shaharuddin, N. M. R., and Mat Darus, I. Z., "Active Vibration Control of Marine Riser. In Conference on Control," Systems and Industrial Informatics, pp. 114–119, 2012.

[12] Pitowarno, E., and Mailah, M. "Robust Motion Control for Mobile Manipulator Using Resolved Acceleration and Proportional-Integral Active Force Control," International Review of Mechanical Engineering, 1(5), pp. 549–558, 2007.

[13] Jamali, A., Darus, I. Z., Mat Samin, P. P., Mohd; Tokhi, M. O., "Intelligent modeling of double link flexible robotic manipulator using artificial neural network.," Journal of Vibroengineering, Vol. 20 Issue 2, pp.1021-1034, Mar 2018.

[14] Saad, M. S., "Evolutionary optimization and real-time self-tuning active vibration control of a flexible beam system," Ph.D. thesis, Faculty of Mechanical Engineering, Universiti Teknologi Malaysia, 2014.

[15] J. Annisa, I. Z. M. Darus, M. O. Tokhi and S. Mohamaddan, "Implementation of PID Based Controller Tuned by Evolutionary Algorithm for Double Link Flexible Robotic Manipulator," *2018 International Conference on Computational Approach in Smart Systems Design and Applications (ICASSDA)*, Kuching, 2018, pp. 1-5.